Optics and Laser Technology 125 (2020) 106028

Contents lists available at ScienceDirect

Optics and Laser Technology

journal homepage: www.elsevier.com/locate/optlastec

The conversion from a Gaussian-like beam to a flat-top beam in the laser hardening processing using a fiber coupled diode laser source

Hongbo Zhu[a,c], Xihong Fu[a], Shengli Fan[c], Lei Liang[a], Xingchen Lin[a,b,*], Yongqiang Ning[a]

[a] State Key Laboratory of Luminescence and Applications, Changchun Institute of Optics, Fine Mechanics and Physics, Chinese Academy of Sciences, No. 3888, Nanhu Road, Changchun 130033, China

[b] Harbin Engineering University, Science College, No. 145, Nantong Road, Harbin 150001, China

[c] CREOL, College of Optics and Photonics, University of Central Florida, Orlando, FL 32816, USA

HIGHLIGHTS

- The beam from diode laser is converted to a flat-top distribution for laser hardening.
- A detailed investigation on HOSs with different parameters are simulated by using ZEMAX.
- A Rockwell hardness of 57 HRC and a hardened depth of 1.6 mm are obtained on 35CrMo metal steel.

ARTICLE INFO

Keywords:
High power
Diode laser
Homogeneity
Laser hardening

ABSTRACT

In this paper, a laser beam from a fiber coupled diode laser source is converted from a Gaussian-like distribution to a flat-top distribution using a set of homogenization optical system, which makes this diode laser source more favorable for laser hardening. Employing this diode laser source, hardening experiments are performed on 35CrMo metal steel. By optimizing parameters of the hardening processing, at the scanning speed of 1100 mm/min and laser power of 1940 W, a Rockwell hardness of 57 HRC and a hardened depth of 1.6 mm are achieved. Experimental results demonstrate the processing ability of this diode laser source in the industrial laser hardening.

1. Introduction

Due to the high rate of heat transfer, low thermal distortion and flexible controllability, the laser hardening has become an important role in the field of the surface treatment [1,2]. In the processing, the laser beam with high power density radiates on the metallic surface, resulting in the surface heated up locally and rapidly cooling by conduction. Then the structure of the metallic material transforms from an austenite into a martensite which is an extremely hard material and desirable in the industry [3]. In the field of the laser hardening, the diode laser source (DLS) has many advantages over Nd:YAG and CO_2 lasers, such as excellent electro-optical efficiency, high absorptivity for metallic materials and low cost [4,5]. Most of all, a natural linear focal beam emitted from the stack-based DLS, with a flat-top distribution in the slow axis and a Gaussian-like distribution in the fast axis, is especially suitable for the laser hardening [6]. The flat-top distribution has a uniform intensity distribution, which can produce a homogeneously hardened area. Because of the high integration density, nevertheless, diode laser stacks usually have an intrinsic defect of poor heat dissipation [7]. This defect can result in the lifetime loss of DLS after it operating for a period of time. Otherwise, “smile effect” inevitably occurred in the soldering process of diode laser bars can cause the deterioration of beam quality and the decrease of power density, which further leads to the low processing efficiency and the production of material defects [8].

With the development of the diode laser technology, DLSs have a significant progress on the output power and beam quality [9,10]. Yielding multi-kW power from an optical fiber makes them suitable for the laser welding and cutting [11,12]. Additionally, this type of DLS has its advantages over stack-based DLS, such as long lifetime, good beam quality and high reliability. Considering the laser hardening, unfortunately, the fiber coupled DLS generally produces a Gaussian-like distributed circular beam with a high intensity at the centre of the beam, decreasing rapidly with the distance from the centre [13]. This

* Corresponding author at: State Key Laboratory of Luminescence and Applications, Changchun Institute of Optics, Fine Mechanics and Physics, Chinese Academy of Sciences, No. 3888, Nanhu Road, Changchun 130033, China.
E-mail address: linxc@ciomp.ac.cn (X. Lin).

https://doi.org/10.1016/j.optlastec.2019.106028
Received 30 June 2019; Received in revised form 11 December 2019; Accepted 20 December 2019
Available online 08 January 2020
0030-3992/

leads to an uneven hardened depth and in extreme cases, surface melting may exist in the centre of the beam whereas the austenitizing temperature has not been reached on the beam perimeter.

To date, much of research on the laser hardening is mainly focused on stack-based DLSs [14]. However, for the fiber coupled DLS, detailed investigation on the beam conversion from a Gaussian-like beam to a flat-top beam in the hardening processing is rarely researched. Thus, this is a limitation for the future development of the diode laser hardening technology. In this work, we employ a DLS which can produce a power of 2045 W from an output fiber with 105 μm core diameter and 0.2 numerical aperture (NA). Using a set of homogenization optical system (HOS), the output beam with a Gaussian-like distribution is converted to a flat-top distribution, which makes this DLS more favorable in the laser hardening. By optimizing processing parameters of the laser hardening, a maximum Rockwell hardness of 57 HRC and a hardened depth of 1.6 mm are obtained on 35CrMo metal steel. This work not only demonstrates the processing ability of a fiber coupled DLS with this power class in the laser hardening, but also provides the experimental guidance for the further research of the diode laser processing.

2. Design of experiments

2.1. Specifications of diode laser source

DLS employed in this work is based on the technology of multi-wavelength multiplexing. Its internal optical structure has been previously introduced in [15], so we briefly describe it here. Compared to the stack-based DLS, unit diode laser devices installed in this source are commercially available diode laser blocks which are manufactured on the technology platform of the single-emitter multiplexing. The single-emitter diode lasers have long lifetime and high beam quality, which eventually leads to the whole DLS with these merits. Using dense spectral multiplexing, five identical diode laser blocks are superposed as a single-wavelength submodule that can produce high output power. With the combination of the polarization multiplexing and coarse spectral multiplexing, three submodules of 91× nm, 94× nm and 97× nm wavelength are superposed together to further improve the output power. Afterwards, the output beam is coupled, by an aspherical lens, into an industrial optical fiber with 105 μm core diameter and 0.2NA. At the cooling temperature of 25 °C and the continuous wave operating mode, a power of 2045 W and an electro-optical efficiency of 42% are obtained at the injection current of 10 A.

2.2. Design of a homogeneous focal beam

In the laser hardening, it is necessary to make multiple passes on the metallic surface if the size of the laser focal beam is not long enough to cover the entire processing area. In this way, the lateral heat input affecting the previous hardened track may cause “back tempering”, which can reduce the hardness of the processing area considerably. Thus, a long enough focal beam with the flat-top distribution is favorable for the laser hardening, which can improve the processing quality, increase the processing efficiency and reduce the impact of the temperature gradient. A HOS is designed to convert the beam with a Gaussian-like distribution to a flat-top distribution [16]. The schematic structure is shown in Fig. 1.

Firstly, the beam emitted from the optical fiber is collimated by a group of triplet lenses with a focal length of 100 mm. The triplet lenses can eliminate the spherical aberration of the beam. The intensity distribution of the beam after collimation is a circular intensity distribution, which is shown in Fig. 4 (a). Correspondingly, the focal beam is Gaussian-like distribution. Thus, a set of HOS consisted of two cylindrical lens arrays (CLAs) and a subsequent field lens with a focal length of 350 mm is utilized to homogenize the focal beam. The principle of the homogenization is that CLAs split the wavefront of the incident

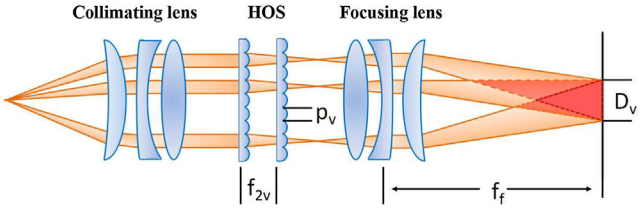

Fig. 1. Schematic diagram of HOS, p_v, f_{2v} and f_f denote the pitch, the focal length of the second CLA and the field lens, respectively. D_V denotes the size of the focal beam.

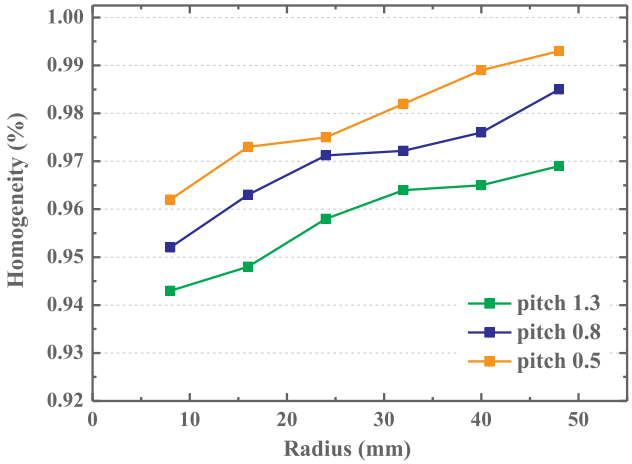

Fig. 2. The homogeneity of the focal beam with varying radius and pitch.

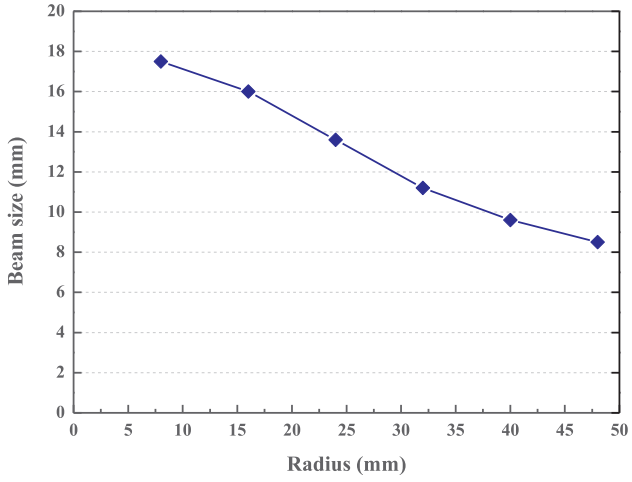

Fig. 3. The homogeneity of the focal beam with the varying radius and pitch.

laser beam into many wavelets, and then the field lens focuses and overlaps these wavelets together. Because CLAs only split the incident laser beam in one direction, a focal beam with a flat-top distribution is obtained, and the beam in the other direction can be focused well into a Gaussian-like distribution. The imaging characteristics of HOS are mainly regulated by the radius of the lens surface and the pitch of cylindrical lenses. The size of the focal beam is calculated by

$$D_v = p_v \times \left(\frac{f_f}{f_{2v}}\right), \tag{1}$$

where p_v, f_{2v}, f_f respectively denotes the pitch, the focal length of the second CLA and the field lens. D_V denotes the size of the focal beam. From Eq. (1) we can see that the size of the focal beam can be controlled by a reasonable design of the radius of surface and the pitch of

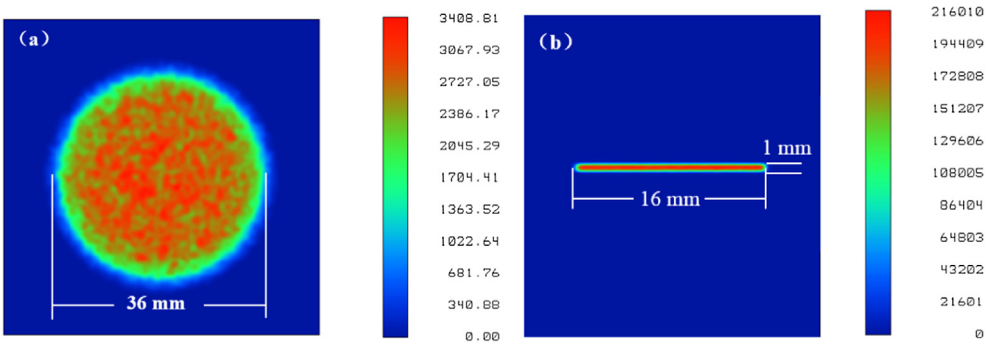

Fig. 4. The intensity distribution of the focal beam after collimation (a) and after HOS (b).

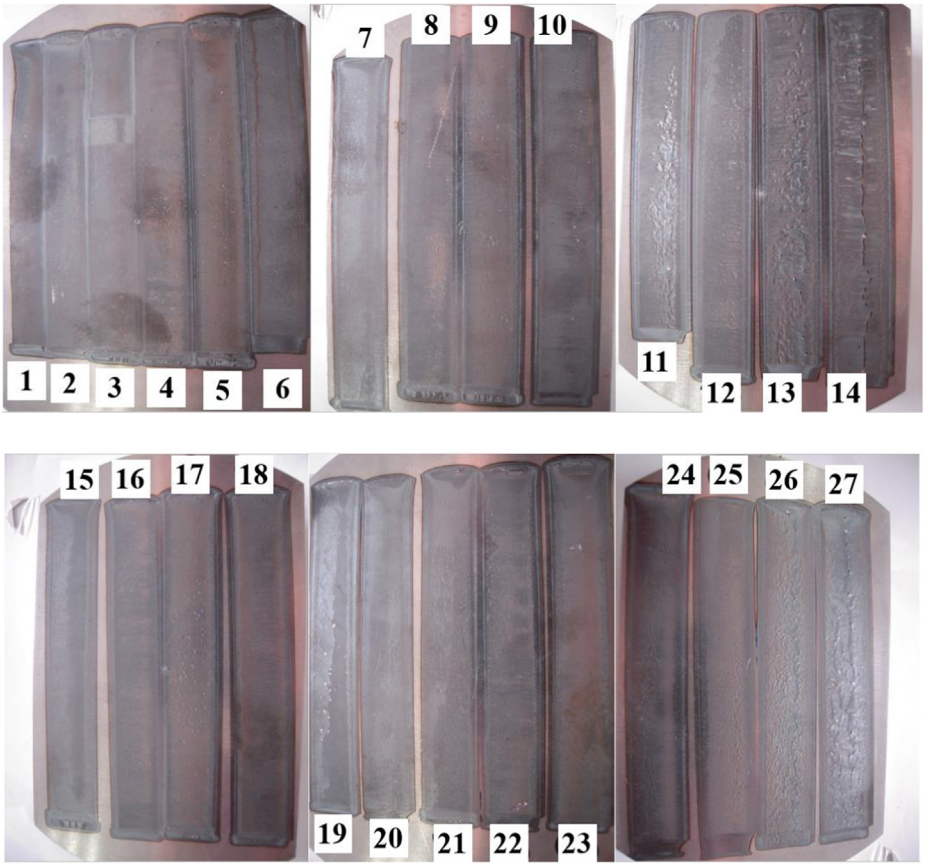

Fig. 5. Specimens of the laser hardening on 35CrMo metal steel.

Table 1
Processing parameters of the laser hardening. The hardness and hardened depth are measured using a Rockwell hardness tester and a microscope.

No.	Laser power (W)	Scanning soeed (mm/min)	Hardness (HRC)	Hardening depth (mm)	Roughness	No.	Laser power (W)	Scanning soeed (mm/min)	Hardness (HRC)	Hardening depth (mm)	Roughness
1	1200	1400	41.5	1.18	excellent	15	1400	1100	45.4	1.38	good
2	1400	1400	42.5	1.30	excellent	16	1600	1100	52.9	1.48	excellent
3	1600	1400	49.7	1.34	excellent	17	1800	1100	56.4	1.54	excellent
4	1800	1400	50.5	1.36	excellent	18	1940	1100	57.0	1.60	excellent
5	1940	1400	52.1	1.40	good	19	1200	1000	44.0	1.28	excellent
6	1400	1300	43.8	1.32	excellent	20	1400	1000	48.4	1.35	unsatisfactory
7	1600	1300	48.2	1.36	excellent	21	1600	1000	55.1	1.46	excellent
8	1800	1300	50.2	1.38	excellent	22	1800	1000	56.1	1.52	poor
9	1940	1300	53.3	1.47	good	23	1940	1000	56.6	1.55	poor
10	1400	1200	49.3	1.37	excellent	24	1400	900	47.5	1.28	excellent
11	1600	1200	53.1	1.43	excellent	25	1600	900	50.5	1.31	excellent
12	1800	1200	54.1	1.48	excellent	26	1800	900	52.8	1.39	poor
13	1940	1200	54.6	1.54	good	27	1940	900	53.0	1.42	poor
14	1200	1100	42.2	1.30	excellent						

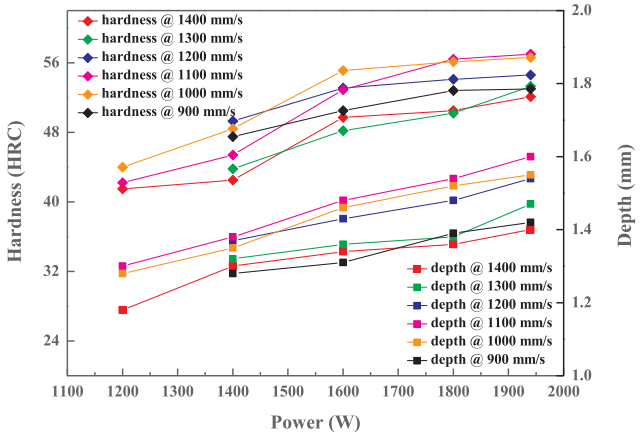

Fig. 6. The hardness of specimens with different power and different scanning speed.

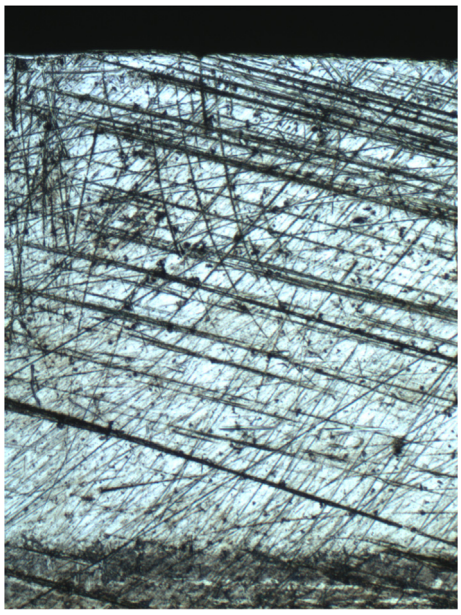

Fig. 7. Cross section of the hardened track on a 35CrMo metal steel.

cylindrical lenses. In this case, HOSs with different surface radius and different pitches are simulated and optimized by using ZEMAX. Meanwhile, the homogeneity of the focal beam is also analyzed. We examine five different radiuses of cylindrical lenses, ranging from 8 mm to 48 mm, in the combination with three different pitches of p = 0.5 mm, 0.8 mm and 1.3 mm, respectively. The material of two CLAs are LAFN21 (n = 1.77), and their size are 50 × 50 mm^2. The homogeneity is used to evaluate the intensity distribution of the focal beam and is defined as

$$V = 1 - \frac{(I_{max} - I_{min})}{(I_{max} + I_{min})}, \quad (2)$$

where I_{max} and I_{min} are the maximum and minimum intensity, respectively. A detailed numerical calculation of the homogeneity has been performed, which is plotted in Fig. 2.

From Fig. 2 we can draw the conclusion that all curves have a similar tendency, at the same radius, smaller pitch can result in a higher homogeneity. For a given pitch, however, the homogeneity displays the increasing tendency with the increasing radius. For instance, with the pitch of 0.5 mm, the homogeneity can gradually increase from 96.1% to 99.2% when the radius increases from 8 mm to 48 mm. Nevertheless, in the laser hardening, the large beam size means the low power intensity. So we should also consider the beam size in the parameter selection. Using Zemax to simulate the influence of the radius on the beam size, we can see that the beam size decreases with the increasing radius, which is shown in Fig. 3.

According to the above analysis, in consideration of the homogeneity and the beam size in the actual processing, the pitch and radius are respectively set to be 0.5 mm and 16 mm in our case. Correspondingly, an effective size of approximate 16 × 1 mm^2 is obtained at the focal plane. The simulation result is shown in Fig. 4 (b). It is noting that the beam is focused to a homogeneous linear shape spot along one direction, simultaneously, the beam along the other direction is focused narrowly.

3. Experiments and results

In the practical experiment, DLS is integrated into an industrial machine. The output fiber of DLS is connected with a processing head where HOS designed above is fixed. High purity argon with a flow rate of 35 l/min is applied as a shielding gas to shield the heat affected zone (HAZ), which can prevent the oxidation from the hardened area. The laser power actually radiated on the workpiece reaches 1940 W. Main loss mechanisms of the laser power can be explained as follows:

The transmission of the laser beam in the processing head leads to a certain power loss, which is mainly because that each surface of optical elements is coated by an antireflective film that has a residual reflectance of 0.3%, and the accumulation of the residual reflectance results in a relatively high loss of approximate 4.5% for the whole optical system.

Due to the imperfection in the processing of CLAs, some laser rays deviate from their expected path after HOS, which can then be cut by the outlet of the processing head.

Generally, the average absorptivity of the metallic surface also plays an important role in the laser processing. It not only directly depends on the wavelength of the incident beam, but also on the incident angle. In [10], author analyzed the relationship between the absorptivity and the incident angle, where in the range of 79° and 82°, the maximum absorptivity can reach up to 50%. In our case, the incident angle is set to be 80°, in consideration of the actual mechanical limitation and avoiding the reflected beam from the metallic surface.

Laser hardening experiments are carried out based on changing the laser power (1200–1940 W) and the scanning speed (900–1400 mm/min) to observe the variation of hardening results. 35CrMo metal steels are placed at the focal plane of DLS. The focal beam with the flat-top distribution is moved multiple times on one specimen, and these tracks are not overlapped in case causing “back tempering” for the previous hardened track. Hardened specimens are shown in Fig. 5, and processing parameters are listed in Table 1.

From the appearance of hardened specimens, we can draw the conclusion that experimental results are in good agreement with simulation results in Zemax. Owing to the homogeneous intensity distribution of the focal beam radiated on the metallic surface, wide strips of hardened tracks are obtained in the processing, and the hardened width is almost uniform. We use a Rockwell hardness tester to measure the surface hardness, and results are plotted in Table 1. The original hardness of the base material is in the range of 20 HRC to 21 HRC, however, now all specimens show the hardness in excess of the base material.

Theoretically speaking, long interaction time and high laser power usually result in a deep hardened depth while the converse results in a shallower hardened depth. However, the long interaction time may cause the melt of metallic surface, which results in an unacceptable surface quality of specimens. It is worth noting in Fig. 6, for a given scanning speed, the hardness and hardened depth gradually increase with the improvement of laser power. Nevertheless, at the same power, with the scanning speed decreases, the gradual increase in the hardened depth and hardness is found. The optimum hardened specimen is

obtained at the power of 1940 W and a scanning speed of 1100 mm/min, correspondingly, the hardness and hardened depth are 57 HRC and 1.6 mm, respectively. Then the tendency changes after this point. The hardness and hardened depth respectively reduce to 53 HRC and 1.42 mm for the power of 1940 W and the scanning speed of 900 mm/min. At this time, the accumulation of input heat in the low speed is likely to melt the metallic surface, as we discussed above, so it is difficult to obtain the satisfactory surface quality. Fig. 7 shows the cross-sectional cut of the optimum hardened specimen, and it is clear to distinguish two different regions of the hardened area and the base material. The darker region below the HAZ is the part of the base material which remains unaffected by the laser radiation.

The width of the actual hardened track (17 mm) deviates from the simulation result in Zemax (16 mm), which can be attributed to following points:

In the process of homogenization, the size of the focal beam is also related to the divergence angel of the incident beam. In the previous simulation, we assume the incident beam is a fully collimated beam. In the actual case, nevertheless, the collimated beam usually has a residual divergence angel, which can cause some deviations from the simulation result.

· In the collimation and focusing of the laser beam, we respectively use a group of triplet lenses to reduce the spherical aberration of the laser beam. So many lenses bring some difficulties to the installation of the lens group, resulting in a longer focal beam than the theoretical value.

4. Conclusion

In this paper, to make the diode laser source more suitable for the laser hardening, a set of HOS has been designed and optimized, which converts the diode laser beam from a Gaussian-like distribution to a flat-top distribution. Using this set of HOS, a linear shape focal beam with a size of 17 × 1 mm^2 and a homogeneous distribution along one direction is realized. By exploring parameters of the hardening processing on 35CrMo metal steel, a hardened track with Rockwell hardness of 57 HRC and hardened depth of 1.6 mm are obtained at the power of 1940 W and the scanning speed of 1100 mm/min. The hardened specimen shows a good surface quality. The experimental results demonstrate that this DLS can meet requirements of the industrial laser hardening. The research in this paper provides a significant method for homogenizing the focal beam in the laser hardening and paves the way for the future research of the diode laser processing.

Funding

National Natural Science Foundation of China (NSFC) (61674149) and Science and Technology Cooperation High-tech Industrialization Project of Jilin Province and Chinese Academy of Sciences (2019SYHZ0017)

Declaration of Competing Interest

The authors declare that they have no known competing financial interests or personal relationships that could have appeared to influence the work reported in this paper.

Acknowledgments

We thank our project partners for the assistance and fruitful discussions.

References

[1] R. Li, Y. Jin, Z. Li, K. Qi, A comparative study of high-power diode laser and CO2 laser surface hardening of AISI 1045 steel, J. Mater. Eng. Perform. 23 (9) (2014) 3085–3091.
[2] M. Merklein, M. Johannes, M. Lechner, A. Kuppert, A review on tailored blanks—Production, applications and evaluation, J. Mater. Process. Technol. 214 (2) (2014) 151–164.
[3] S. Santhanakrishnan, F. Kong, R. Kovacevic, An experimentally based thermo-kinetic hardening model for high power direct diode laser cladding, J. Mater. Process. Technol. 211 (7) (2011) 1247–1259.
[4] U. Witte, F. Schneider, M. Traub, D. Hoffmann, S. Drovs, T. Brand, A. Unger, kW-class direct diode laser for sheet metal cutting based on DWDM of pump modules by use of ultra-steep dielectric filters, Opt. Express 24 (20) (2016) 22917–22929.
[5] P. Crump, G. Blume, K. Paschke, R. Staske, A. Pietrzak, U. Zeimer, S. Einfeldt, A. Ginolas, F. Bugge, K. Häusler, P. Ressel, H. Wenzel, G. Erbert, 20W continuous wave reliable operation of 980nm broad-area single emitter diode lasers with an aperture of 96um, SPIE2009.
[6] H. Zhu, M. Hao, J. Zhang, W. Ji, X. Lin, J. Zhang, Y. Ning, Development and thermal management of 10kW CW, direct diode laser source, Opt. Laser Technol. 76 (2016) 101–105.
[7] D. Schröder, J. Meusel, P. Hennig, D. Lorenzen, M. Schröder, R. Hülsewede, J. Sebastian, Increased power of broad-area lasers (808nm/980nm) and applicability to 10-mm bars with up to 1000Watt QCW, SPIE2007.
[8] J.F. Monjardin, K.M. Nowak, H.J. Baker, D.R. Hall, Correction of beam errors in high power laser diode bars and stacks, Opt. Express 14 (18) (2006) 8178–8183.
[9] Y. Sun, K. Zhou, M. Feng, Z. Li, Y. Zhou, Q. Sun, J. Liu, L. Zhang, D. Li, X. Sun, D. Li, S. Zhang, M. Ikeda, H. Yang, Room-temperature continuous-wave electrically pumped InGaN/GaN quantum well blue laser diode directly grown on Si, Light Sci. Appl. 7 (1) (2018) 13.
[10] Y. Mei, G.-E. Weng, B.-P. Zhang, J.-P. Liu, W. Hofmann, L.-Y. Ying, J.-Y. Zhang, Z.-C. Li, H. Yang, H.-C. Kuo, Quantum dot vertical-cavity surface-emitting lasers covering the 'green gap', Light: Sci. Appl. 6 (2017) e16199.
[11] J.A. Alcock, B. Baufeld, Diode laser welding of stainless steel 304L, J. Mater. Process. Technol. 240 (2017) 138–144.
[12] G. Costa Rodrigues, J. Pencinovsky, M. Cuypers, J.R. Duflou, Theoretical and experimental aspects of laser cutting with a direct diode laser, Opt. Lasers Eng. 61 (2014) 31–38.
[13] X. Lin, P. Wang, Y. Zhang, Y. Ning, H. Zhu, Theoretical and experimental aspects of laser cutting using direct diode laser source based on multi-wavelength multiplexing, Opt. Laser Technol. 114 (2019) 66–71.
[14] F. Wang, L. Zhong, X. Tang, C. Xu, C. Wan, A homogeneous focusing system for diode lasers and its applications in metal surface modification, Opt. Laser Technol. 102 (2018) 197–206.
[15] H. Zhu, X. Lin, Y. Zhang, J. Zhang, B. Wang, J. Zhang, L. Qin, Y. Ning, H. Wu, kW-class fiber-coupled diode laser source based on dense spectral multiplexing of an ultra-narrow channel spacing, Opt. Express 26 (19) (2018) 24723–24733.
[16] N. Yeh, Optical geometry approach for elliptical Fresnel lens design and chromatic aberration, Sol. Energy Mater. Sol. Cells 93 (8) (2009) 1309–1317.